


2002

Atomic Hydrogen Cleaning of InP(100): Electron Yield and Surface Morphology of Negative Electron Affinity Activated Surfaces

M. A. Hafez
Old Dominion University

H. E. Elsayed-Ali
Old Dominion University, helsayed@odu.edu

Follow this and additional works at: https://digitalcommons.odu.edu/ece_fac_pubs

 Part of the [Atomic, Molecular and Optical Physics Commons](#), [Electrical and Computer Engineering Commons](#), [Materials Science and Engineering Commons](#), and the [Quantum Physics Commons](#)

Repository Citation

Hafez, M. A. and Elsayed-Ali, H. E., "Atomic Hydrogen Cleaning of InP(100): Electron Yield and Surface Morphology of Negative Electron Affinity Activated Surfaces" (2002). *Electrical & Computer Engineering Faculty Publications*. 103.
https://digitalcommons.odu.edu/ece_fac_pubs/103

Original Publication Citation

Hafez, M. A., & Elsayed-Ali, H. E. (2002). Atomic hydrogen cleaning of InP(100): Electron yield and surface morphology of negative electron affinity activated surfaces. *Journal of Applied Physics*, 91(3), 1256-1264. doi:10.1063/1.1429796

Atomic hydrogen cleaning of InP(100): Electron yield and surface morphology of negative electron affinity activated surfaces

M. A. Hafez and H. E. Elsayed-Ali^{a)}

Department of Electrical and Computer Engineering and the Applied Research Center, Old Dominion University, Norfolk, Virginia 23529

(Received 16 July 2001; accepted for publication 1 November 2001)

Atomic hydrogen cleaning of the InP(100) surface has been investigated using quantitative reflection high-energy electron diffraction. The quantum efficiency of the surface when activated to negative electron affinity was correlated with surface morphology. The electron diffraction patterns showed that hydrogen cleaning is effective in removing surface contaminants, leaving a clean, ordered, and (2×4) -reconstructed surface. After activation to negative electron affinity, a quantum efficiency of $\sim 6\%$ was produced in response to photoactivation at 632 nm. Secondary electron emission from the hydrogen-cleaned InP(100)- (2×4) surface was measured and correlated to the quantum efficiency. The morphology of the vicinal InP(100) surface was investigated using electron diffraction. The average terrace width and adatom-vacancy density were measured from the (00) specular beam at the out-of-phase condition. With hydrogen cleaning time, there was some reduction in the average terrace width. The surface quality was improved with hydrogen cleaning, as indicated by the increased (00) spot intensity-to-background ratio at the out-of-phase condition, and improved quantum efficiency after activation to negative electron affinity. © 2002 American Institute of Physics. [DOI: 10.1063/1.1429796]

I. INTRODUCTION

Indium phosphide is a material of considerable importance in the area of developing electronic and optoelectronic devices. InP-based high electron mobility transistors are attractive for low noise, high power, and high speed applications.¹ Preparation of a high quality InP surface is an important step prior to epitaxial growth. Surface defects lead to thin film and interface quality degradation in the growth of heterostructures. Surface cleaning at low substrate temperatures is an essential step to eliminate the interface carrier depletion region and minimize defect-induced surface states.

InP is used for negative electron affinity (NEA) device fabrication; consequently, preparation of a clean surface is required in order to reduce the density of surface states. Surface contamination produces lower quantum efficiency (QE) photocathodes. The main contaminants observed on InP surfaces are carbon and oxygen.² Chemical cleaning alone does not provide a carbon-free surface.³ Native oxides are desorbed by heating to ~ 500 – 530 °C, a temperature much higher than the InP congruent temperature (~ 400 °C) at which the phosphorus atoms desorb preferentially, leaving an indium-rich rough surface with poor electronic quality.^{4,5} Adsorbed carbon is strongly bonded to III–V surfaces and remains on the surface even after annealing under phosphine overpressure at high temperatures.⁶

There is a considerable interest in developing methods of producing clean InP surfaces while avoiding phosphorus loss, which leads to creation of electronic defects. Surface cleaning of InP and GaAs using atomic hydrogen was

studied.^{2,5,7} Atomic hydrogen cleaning is used for substrate preparation before epitaxial growth^{7,8} or activation to NEA.⁹ The main advantages of this technique are the low cleaning temperature and the avoidance of degradation to the surface electronic properties, which occurs in hydrogen plasma cleaning due to the presence of energetic ions (up to ~ 100 eV) that cause surface damage. The interaction of atomic hydrogen with semiconductor surfaces has been the subject of many studies.^{10–12} Atomic hydrogen cleaning of III–V semiconductors has been reported using rf discharge,⁷ electron cyclotron resonance discharge,¹³ and a thermal cracking source.² Thermal sources produce hydrogen radicals with kinetic energies typically less than 1 eV,¹⁴ thus, atomic hydrogen interaction is limited to the surface top layer. Exposure to atomic hydrogen removes surface contaminants and blocks the electrical activity of dangling bonds.⁴ Atomic hydrogen reacts with the stable In oxide, In_2O_3 , and lowers the cleaning temperature by producing a more volatile In oxide, In_2O .² Auger analysis of InP surfaces shows complete removal of carbon and oxygen after hydrogen cleaning.² The dissociative adsorption of NH_3 and SiH_4 on InP surfaces was studied.^{15,16} It was shown that it takes much longer irradiation time to clean the InP surface than it takes for cleaning the GaAs surface.⁵ For InP, atomic hydrogen cleaning can be accomplished at a surface temperature ~ 350 – 400 °C.⁹ This process is limited by the removal of hydrocarbons, which persist at high temperatures, and the relatively high temperature needed to remove indium phosphate, $\text{In}(\text{PO}_3)_3$.⁵

Reflection high-energy electron diffraction (RHEED) is a useful *in situ* technique to study surface morphology. Surface processes such as thin film growth, phase transformation, and changes in surface morphology can be investigated by quantitative RHEED.¹⁷ The surface we studied was a vicinal

^{a)} Author to whom correspondence should be addressed. Electronic mail: helsayed@odu.edu

nal InP(100). A vicinal surface is slightly inclined to a low-index surface.^{18,19} When the electron beam is incident down the staircase, the RHEED pattern is modified by the step structure, and a splitting specular beam is obtained at the out-of-phase condition. In this case, the RHEED pattern is most sensitive to surface defects. Surface terrace width and terrace width distribution of the vicinal surface can be measured from the split peak spacing and their widths at the out-of-phase condition.¹⁷ The split peak spacing depends on the incident electron beam angle relative to the staircase direction. RHEED was previously used to study surface cleaning of hydrogen-plasma treated GaAs and Si surfaces.²⁰

A surface with NEA is obtained when the vacuum level is lowered below the bulk conduction band minimum at the surface; thus, electrons excited to the conduction band minimum can be emitted from the surface. The escape depth in this case is not limited by the mean-free path of the hot electrons, which is on the order of 10 nm, but by the diffusion length of the electrons thermalized to the conduction band minimum, which is on the order of several μm .²¹ Achieving NEA requires the combination of electron affinity lowering and downward band bending,²² and thus *p*-type doping is favored. Quantum efficiency and high secondary emission are obtained as a result of the surface NEA and the long escape depth of photoelectrons and internal secondaries.²³ Hydrocarbons and oxides present on the surface establish a surface energy barrier. For GaAs, air-exposed surfaces are known to contain a high density of surface states which pin the surface Fermi level at midgap.²⁴ Thus, cleaning is a required step in preparing NEA surfaces.

We have prepared NEA InP(100) surfaces by surface cleaning with atomic hydrogen and then activating to NEA by alternate exposure to oxygen and cesium.⁹ Here, we extend this work to study the effect of atomic hydrogen cleaning on surface morphology such as surface terrace width and vacancy-adatom density. RHEED was used to monitor the development of the surface morphology with atomic hydrogen cleaning time. The secondary electron emission from the hydrogen-cleaned InP(100)-(2 \times 4) surface was also measured. The QE and secondary yield were shown to increase with hydrogen cleaning. We have previously used RHEED to study the surface morphology of hydrogen-cleaned GaAs(100) surface.²⁵ In the present work, we use RHEED to investigate the morphology of the InP(100) vicinal surface when heat cleaned at $\sim 300^\circ\text{C}$ and after hydrogen cleaning at $\sim 380^\circ\text{C}$. Results show that removal of contaminants by atomic hydrogen and the accompanied morphology changes improve the electronic surface quality. Correlation between the measured QE and secondary electron yield with surface morphology as detected with RHEED is shown.

II. EXPERIMENT

The InP(100) wafers used in the present study were *p*-type Zn doped to provide a carrier density of $3 \times 10^{18} \text{ cm}^{-3}$. The wafers had an etch pit density $< 500 \text{ cm}^{-2}$ as determined by the manufacturer. The samples were not chemically etched, but only degreased in ethanol before loading in the ultrahigh vacuum (UHV) chamber. The cham-

ber was baked out after loading the sample. The experiments were carried out in a stainless-steel UHV chamber pumped by a 220 l/s ion pump. A titanium sublimation pump was also used to reduce the base pressure. The InP wafer was mounted on a molybdenum plate on top of a resistive heater that can be heated to 600°C . The sample was fixed with two molybdenum clamps. A thermocouple was attached to the sample holder close to the sample in order to measure its temperature. A wire was connected to the sample holder to apply a negative voltage bias to the sample for photocurrent measurement. The sample holder was connected to a *xyz* manipulator through a ceramic rod that electrically insulated the sample from the chamber walls, which was used as the anode for the negatively biased InP substrate. The manipulator provided azimuthal rotation, in order to set the direction of the incident electron beam when acquiring the RHEED patterns. A schematic of the UHV chamber was previously shown.⁹ The substrate faced a processing port, containing a cesium source, a leak valve for oxygen admission, a glass window to allow the laser light to activate the InP photocathode, and a port for the hydrogen cracker source. The RHEED patterns were acquired by a charge coupled device (CCD) detector connected to a computer and a video monitor. Calibration of the scaling constants from CCD pixels to reciprocal space units was carried out. The surface of the sample was raised to the desired temperature by the resistive heater and then exposed to atomic hydrogen. The hydrogen cracker source consists of a tungsten filament inserted into an 80-mm-long boron nitride tube with 4 mm inner diameter. The temperature of the filament was maintained $\sim 2000^\circ\text{C}$, as measured by a pyrometer. Molecular hydrogen was introduced through a leak valve and passed in the boron nitride tube where it becomes partially dissociated and the produced atomic hydrogen was transported to the sample. The dissociation efficiency, based on the filament temperature, was estimated to be $\sim 3\%$.²⁶

III. RESULTS AND DISCUSSION

A. Quantum efficiency and secondary electron emission

The preparation of a NEA InP(100) surface was initiated by cleaning in UHV. The chamber was baked for ~ 48 h to attain a base pressure of $\sim 1 \times 10^{-10}$ Torr, while the InP sample was kept at $\sim 350^\circ\text{C}$ during baking to reduce surface contamination. RHEED was used to monitor the effect of heat and atomic hydrogen cleaning on the InP(100) surface. The incident electron energy was 9 keV. Activation to NEA was performed, while the sample was at room temperature. The standard method of activation to NEA by alternate deposition of cesium and oxygen according to the *yo-yo* procedure was followed.²⁷ Before surface cleaning, the RHEED pattern showed a halo indicative of a surface covered with hydrocarbons and native oxides.

The sample cleaning was performed in several 3 h cycles. The QE and the secondary electron emission (SEE) were measured after cooling the sample to room temperature (RT) and activating the surface to NEA. The SEE was measured by directing the primary RHEED gun electron beam

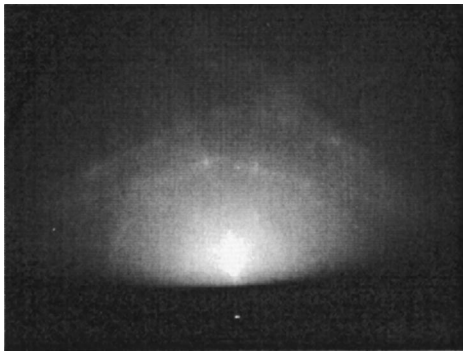


FIG. 1. RHEED patterns of InP(100) surface after heat cleaning at 370 °C showing a strong background due to contaminants.

onto the surface at an angle of $\sim 3.5^\circ$. The resulting SEE current was measured before and after activation, and the ratio between the two currents is given as the SEE ratio ($I_{\text{activated}}/I_{\text{nonactivated}}$). A negative bias of ~ 100 V was applied to the sample when measuring electron emission. During cleaning, the hydrogen pressure inside the chamber was $\sim 4 \times 10^{-6}$ Torr and the cracker source was operated at ~ 2000 °C.

In the first cycle, the sample temperature was raised gradually under vacuum at a rate of 4–7 °C/min to ~ 370 °C and held at that temperature for 3 h. The sample was then cooled to RT and activated to NEA. A QE of $\sim 0.2\%$ was obtained in response to 632.8 nm light. Some diffraction features of the RHEED pattern could be seen. Figure 1 shows the RHEED pattern obtained after heat cleaning at ~ 370 °C. No photoemission can be measured when the same activation procedure is performed on a surface that has not been heat cleaned. In another sample, heat cleaning at ~ 300 °C followed by activation to NEA resulted in a QE of $\sim 0.1\%$.

In the following cycles, the temperature of the sample was raised to the desired value, also at a rate of 4–7 °C/min, and then the surface was exposed to atomic hydrogen for 3 h in each cycle. Figure 2 shows the measured QE and SEE ratio obtained at RT for a NEA InP(100) surface after a se-

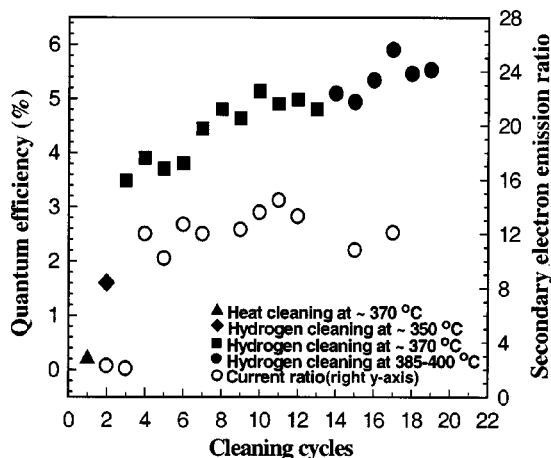


FIG. 2. The quantum efficiency and secondary electron emission ratios were measured for a (2×4)-reconstructed InP surface. At each cleaning cycle, the InP sample was cleaned for 3 h and the measurements were taken at room temperature.

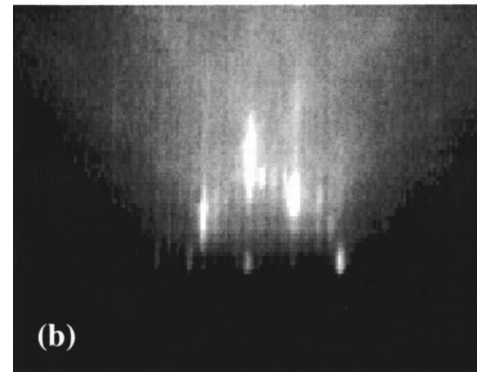
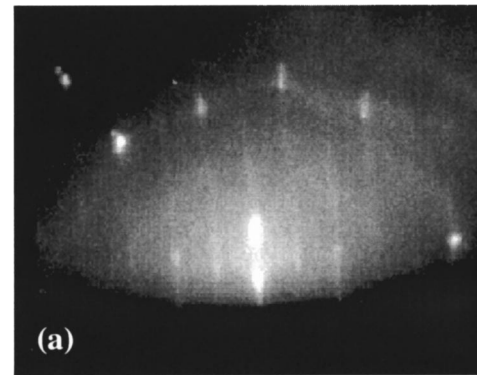


FIG. 3. RHEED patterns of InP(100) surface after atomic hydrogen cleaning. (a) After hydrogen cleaning at ~ 370 °C, the RHEED streaks are visible along with a strong background. The electron beam was incident along the [031] direction. (b) After hydrogen cleaning at 385–400 °C, a clear (2×4)-reconstructed surface is obtained. The electron beam was incident along the [011] direction.

quence of surface cleaning. The data points in Fig. 2 were obtained successively on the same sample that was first subjected to a 3 h heat cleaning indicated in Fig. 2 as cycle 1. Cycles 2–19 were all hydrogen cleaning 3 h cycles at the indicated sample temperature.

In the second cleaning cycle, the sample temperature was raised to ~ 350 °C and then exposed to atomic hydrogen. After activation to NEA, a QE of 1.6% was obtained and the measured SEE ratio was ~ 2.3 . The RHEED patterns obtained before activation to NEA showed streaks with large background, indicating the presence of surface contaminants. These contaminants result in a surface interfacial barrier reducing the QE. After activation, the RHEED streak intensity decreased with cesium deposition because cesium adsorbs on the surface in a fashion that lacks long-range order. Atomic hydrogen exposure was effective in removing cesium and surface contaminants improving the surface electronic quality.

In cycles 3–13, we further exposed the sample to atomic hydrogen while its temperature was kept at ~ 370 °C. After the third hydrogen cleaning cycle, a QE of 3.9% was produced and the SEE ratio increased to ~ 12 . In addition, a clear streaky RHEED pattern was observed with low background intensity. Figure 3(a) is an example of a RHEED pattern obtained after a few hydrogen cleaning cycles at ~ 370 °C with the electron beam incident along the [031] direction. The RHEED pattern showed noticeable improve-

ment after the surface temperature was raised to 370 °C and was exposed to atomic hydrogen. However, only gradual changes in the pattern were observed with increased hydrogen cleaning time at ~370 °C (cleaning cycles 3–13 in Fig. 2). The improvement in QE and SEE ratio is expected to be due to the removal of oxides and carbon atoms during InP surface cleaning. When the azimuthal direction of the sample was changed relative to the primary electron beam, there was no significant change in the resultant secondary emission current. After cleaning cycle 10, the QE increased to ~5%. An $I_{\text{activated}}$ of ~113 μA was measured after activating the sample to NEA, and a SEE ratio of ~13 was obtained. An increase in the hydrogen cleaning time improved electron yield to a saturation level, which depended on the surface cleaning temperature and on other conditions such as the sample used, its processing history, and the vacuum condition.

In cycles 14–19, the sample was heated to 385–400 °C and then exposed to atomic hydrogen. At cleaning cycle 17, the QE increased to ~6% in response to 632.8 nm light. There was no further increase, however, in the SEE ratio after hydrogen cleaning at 385–400 °C, as shown in Fig. 2. We have previously observed QE as high as ~8.5% on an InP(100) NEA surface.⁹ The maximum achieved quantum efficiency is highly sensitive to sample preparation and the vacuum condition. In the present work, we focused on the surface morphology of InP(100) with atomic hydrogen cleaning rather than optimizing the QE. Also, changes in the surface morphology were monitored by electron diffraction for a relatively long atomic hydrogen cleaning time.

A high-quality InP(100) surface can be obtained with atomic hydrogen cleaning. Figure 3(b) is a RHEED pattern obtained after hydrogen cleaning at 385–400 °C, showing the quarter-order streaks of the clean phosphorus-stabilized (2×4)-reconstructed surface. The electron beam was incident along the [0 $\bar{1}$ 1] direction. The presence of well-defined diffraction spots falling on semicircles indicates that the oxides on the surface were removed with little surface damage. In addition, Kikuchi lines can be seen from the RHEED pattern, which indicates the high quality of the crystal below the top layers.

Surface and bulk properties affect the SEE ratio and QE. In Fig. 4, two sets of data are shown for the SEE ratio. Each of these sets was acquired at different surface preparation conditions resulting in different QE when exposed to 632.8 nm. The secondary electron yield from cesium covered InP(100) surface was observed to depend on the surface quality as well as the primary electron energy. The SEE ratio increased with the incident electron energy, although some saturation was observed at the higher incident electron energies (>6 keV). A higher SEE ratio was obtained for the surface that produced higher QE. This SEE ratio was obtained for a 3.5–9.5 keV electron beam incident on the InP(100) surface at an angle of ~3.5°. The grazing angle of incidence was used because it can be obtained with the RHEED gun. Secondary electron emission from NEA-activated semiconductor surfaces such as Si and GaAs was measured before.^{23,28,29} Results on a thin epitaxially grown *p*-doped GaAs(100) surface show a SEE of 400 for a primary

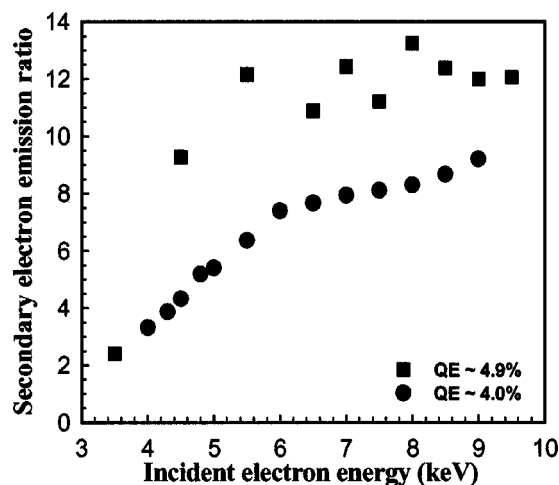


FIG. 4. After activating the surface with cesium and oxygen, the secondary electron emission increased with the incident electron energy. The secondary-electron yield is higher for a surface that produces higher quantum efficiency.

electron energy of 20 keV incident normal to the surface.²⁸ The electron escape depth was estimated to be 2 μm and a surface escape probability of 0.14. The grazing angle of the primary electrons in our experiment reduces their range by $\sin \theta_i$, where θ_i is the primary electron angle of incidence. Thus, in our geometry the range of the primary electron is ~0.06 of that for normal incidence which we expect to be the reason for the low SEE observed in our case.

After activating the InP surface to NEA, the secondary electrons were observed to decrease with time, as shown in Fig. 5. The secondary emission decreased to ~65% of its maximum value after ~20 min, which was at a faster rate than we observe for QE decay.⁹ This could be due to accelerated desorption of cesium from the InP surface due to electron stimulated desorption by the high-energy primary electrons. In our case, cesium was deposited alternately with oxygen until the highest QE was achieved, at which point the SEE ratio was also observed to reach its maximum. As the optimum cesiation degrades by desorption, for example, the

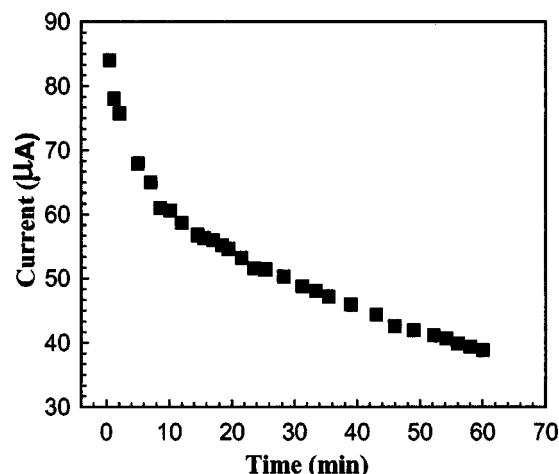


FIG. 5. The decrease of secondary electron emission with time after InP(100) surface activation to NEA. The measurement was taken after atomic hydrogen cleaning at ~370 °C.

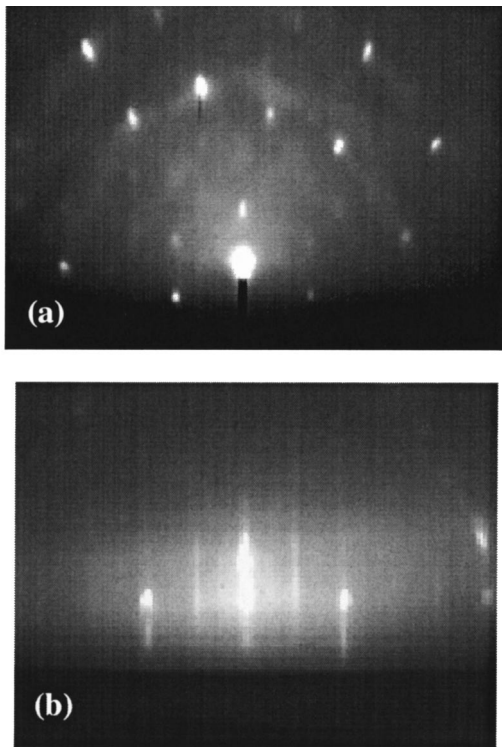


FIG. 6. After several hydrogen cleanings at $\sim 385\text{--}400^\circ\text{C}$, spotty and streaky RHEED patterns were observed at different locations as shown in (a) and (b), respectively. The electron beam was incident along the $[031]$ direction.

number of secondary electrons able to escape from the surface is reduced. We also note that the life of the photocathode has a strong dependence on the vacuum level and processing history of the sample.

After six cleaning cycles at $385\text{--}400^\circ\text{C}$, the RHEED pattern features were observed to depend on the position of the incident electron beam on the sample. When the electron beam was incident along the $[031]$ direction near the center of the sample, a spotty RHEED pattern appeared. Directing the 632.8 nm light to this location produced a QE of $\sim 1.8\%$. Close to the sample edge, the RHEED pattern showed a streaky surface. At this location, a QE of $\sim 2.3\%$ was obtained. Those RHEED features can be seen in Figs. 6(a) and 6(b). As seen from the diffraction patterns, the surface structure became nonuniform over the surface area. Thus, the InP surface decomposed to form phosphorus vapor leaving indium droplets at certain locations of the InP surface. This was also evident from the increase in the vacuum chamber pressure. Since there was some temperature variation on the surface, we expect that this variation caused the nonuniform decomposition of the InP surface. When phosphorus is desorbed from the InP surface leaving vacant sites, surface defects are created, therefore, a rough surface is produced with poor electronic properties and low QE. With additional cleaning cycles, transmission RHEED patterns were observed all over the sample area. In addition, the base pressure of the chamber which was $\sim 1 \times 10^{-10}$ Torr increased to the low 10^{-9} Torr range. Prolonged heating at $385\text{--}400^\circ\text{C}$ during hydrogen cleaning resulted in desorption of phosphorus leaving an indium-rich surface.

Hydrogen cleaning in all the above reported measurements was performed at temperatures of $\sim 370^\circ\text{C}$ or higher. Atomic hydrogen cleaning at lower temperatures is less effective.⁹ For InP and GaAs, some sample heating to a temperature below the congruent temperature, at which P or As desorb preferentially leaving a damaged surface, is needed to prepare a clean reconstructed surface with high QE.^{9,25} The higher the sample temperature up to the observation of surface damage, the higher the QE after activation to NEA. Repetitive hydrogen cleaning treatment cycles were used in order to show the time progression of the cleaning process. For actual device fabrication, only one hydrogen cleaning period at a temperature close, but less than, the congruent temperature is required. We have observed previously that this cleaning method generally gives the highest QE.⁹ Improvement in the hydrogen cracker efficiency and atomic hydrogen delivery to the surface can significantly reduce the preparation time.

B. RHEED study of surface morphology

We next discuss a quantitative RHEED study of surface morphology of heat-cleaned and hydrogen-cleaned InP(100) surfaces. The morphology studies were conducted on a new sample cut from the same wafer. After each surface cleaning, the RHEED images were evaluated at RT. The sample was then activated and the QE measured. When the InP sample was heat cleaned at $\sim 300^\circ\text{C}$ for 3 h and then cooled to RT, low intensity diffraction streaks with large background could be seen at different azimuthal directions. Figure 7 shows the angular distribution of the (00) specular beam intensity with the electron beam incident along the $[031]$ direction. The RHEED intensity profiles show a modulated intensity distribution that depends on the electron beam angle of incidence θ_i . At the Bragg (in-phase) condition the perpendicular momentum transfer ($q_\perp = 2k \sin \theta_i$) is an even number of the inverse monolayer step height ($q_\perp = 2n\pi/d$), where n is an integer, d is the monolayer step height, and k is $2\pi/\lambda$. At the in-phase condition, the scattered electrons interfere constructively. Examples of that are shown in Fig. 7 at $\theta_i = 1.9^\circ$ and 3.1° . The out-of-phase condition is obtained when $q_\perp = (2n+1)\pi/d$. At this condition, electrons scattered from different surface layers interfere destructively (an example is shown in Fig. 7 at $\theta_i = 2.2^\circ$). The RHEED pattern in Fig. 7 shows a sharp specular spot at the in-phase condition and a broadened split peak at the out-of-phase condition, which is indicative of regular steps from a vicinal surface.¹⁷ For angles between that satisfying the in-phase or out-of-phase conditions, the intensity of the two peaks in the split specular beam are unequal. An example of that is shown in Fig. 7 at $\theta_i = 2.0^\circ$. Observation of the split specular beam depended on the azimuthal direction of the incident electron beam. When the incident electron beam was directed along the $[0\bar{1}\bar{3}]$ direction, a split peak was also observed in the specular beam. The measured RHEED rocking curve for the specular beam at the $[0\bar{1}\bar{3}]$ direction obtained at RT is shown in Fig. 8. An out-of-phase condition is achieved at an electron angle of incidence $\theta_i \sim 2.1^\circ$. At $\theta_i \sim 3.4^\circ$, the intensity has a maxi-

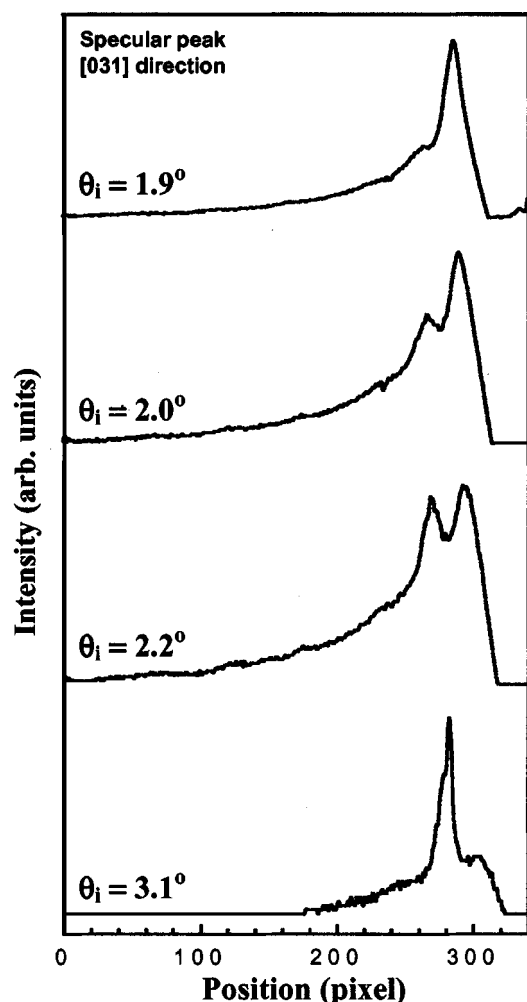


FIG. 7. Intensity profiles along the specular RHEED spot showing the in-phase and out-of-phase conditions. The electron beam was incident along the [031] direction.

mum. At this angle, the incident electron beam penetrates deeper into the InP sample and the bulk Kikuchi-like scattering effects contribute to the intensity.

The terrace width and the split peak profiles of the studied InP(100) surface after heat cleaning at $\sim 300^\circ\text{C}$ were investigated. For terrace width measurement, the electron beam was incident along the [031] direction at which the split specular beam was clearest compared to other azimuthal directions. All RHEED measurements were obtained at RT. The average terrace width for a vicinal surface is determined by the amount of surface misorientation from a low-index plane.³⁰ The split peak spacing is given by $2\pi/L$, where L is the average separation of terraces. The angle $d\theta$ between the specular split peaks was about 14 mrad. Taking into account the instrumental response of $0.89 \pm 0.06 \text{ \AA}^{-1}$, the average terrace width of the heat-cleaned InP(100) vicinal surface was obtained to be $301 \pm 96 \text{ \AA}$. For a single-layer step height ($d=1.468 \text{ \AA}$), the misorientation angle is approximately 0.3° . The instrumental response was obtained from the full width at half maximum (FWHM) along the specular beam at the in-phase condition. The FWHM was measured after subtracting the background, due to inelastic scattering. The intensity profile of the split peaks for the heat-cleaned surface

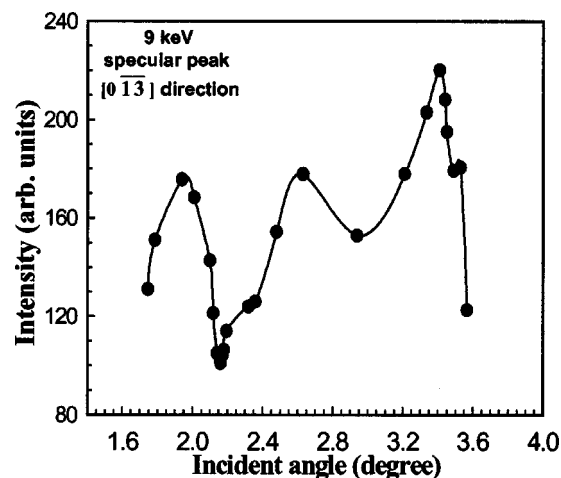
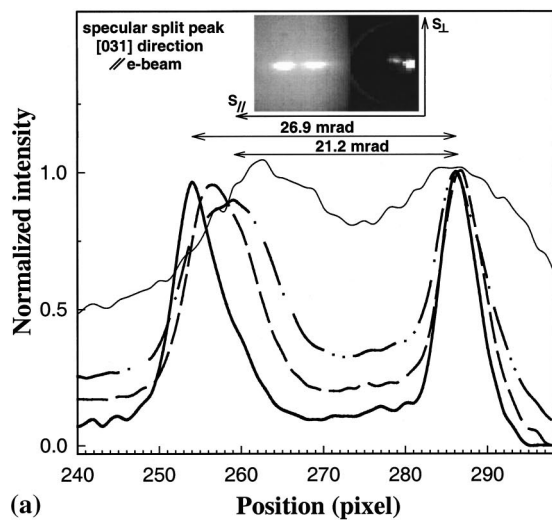


FIG. 8. RHEED rocking curve of the peak intensity of the specular spot for the heat-cleaned vicinal InP(100) surface at $\sim 300^\circ\text{C}$. The intensity profile was obtained close to room temperature in the $[0\bar{1}\bar{3}]$ direction.

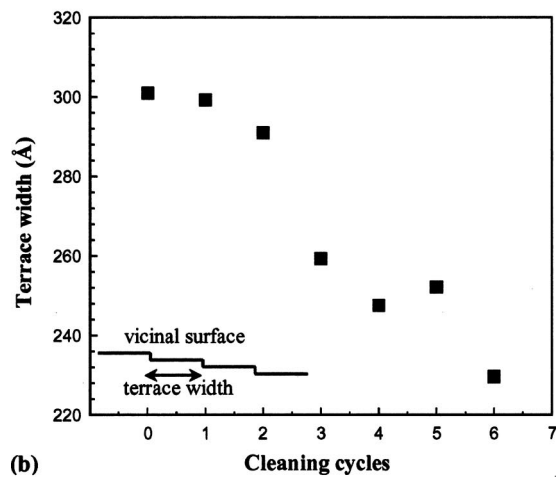
at $\sim 300^\circ\text{C}$ shows high background and is broadened along and across the (00) beam, when observed at the out-of-phase condition. After the first activation to NEA, the heat-cleaned surface produced a QE of $\sim 0.1\%$.

Next, the InP sample was exposed to atomic hydrogen for 3 h cleaning cycles while the sample was kept at $\sim 380^\circ\text{C}$. A clear RHEED pattern at the out-of-phase condition was obtained after cooling the sample to RT. At the out-of-phase condition, the splitting angle $d\theta$ was 20.6 mrad. At the in-phase condition, the instrumental response was $0.66 \pm 0.052 \text{ \AA}^{-1}$. After one 3 h cycle of hydrogen cleaning, the average terrace width of the InP surface was obtained to be $299 \pm 42 \text{ \AA}$, and the background of the RHEED pattern decreased, indicating reduction in surface contaminants. Moreover, the broadening along the split specular peak at the out-of-phase condition was less than before hydrogen cleaning. The QE of the activated surface increased from $\sim 0.1\%$ to 1.4% after the first hydrogen cleaning cycle which was performed at 380°C .

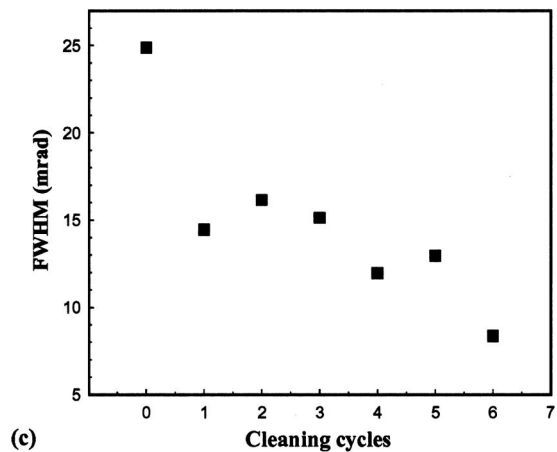
The out-of-phase diffraction was used to evaluate the development of surface morphology with hydrogen cleaning. Following each hydrogen cleaning cycle at $\sim 380^\circ\text{C}$, the average terrace width was measured after allowing the sample to cool to RT. Figure 9(a) shows the RHEED intensity profiles along the (00) specular beam at the out-of-phase condition after different cleaning cycles. The inset of the Fig. 9(a) is a RHEED image of the split peak, where S_{\parallel} and S_{\perp} are the components of the momentum transfer parallel and perpendicular to the electron beam, respectively. The incident electron beam was along the [031] direction. The split peak spacing was observed to increase with cleaning cycles, indicating that the average terrace width of the InP surface was reduced. After the second hydrogen cleaning cycle, an average terrace width of $291 \pm 67 \text{ \AA}$ was obtained. With additional hydrogen cleaning cycles, further decrease in the average terrace width was observed reaching $229 \pm 20 \text{ \AA}$ after hydrogen treatment at $\sim 380^\circ\text{C}$ (cycles 1–6), as shown in Fig. 9(b). For each point, the RHEED intensity profiles were taken four to five times, and the average value was recorded. The errors indi-



(a)

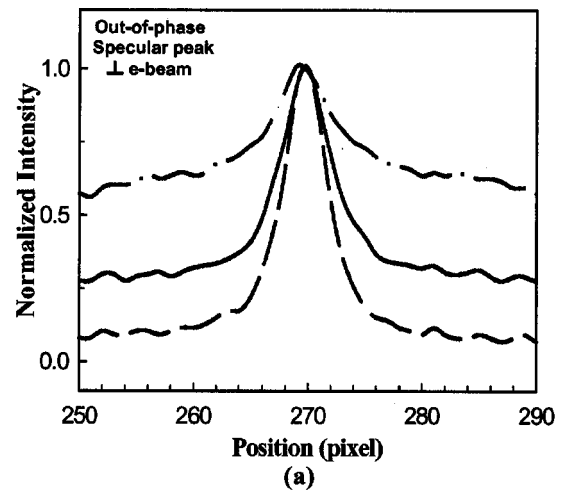


(b)

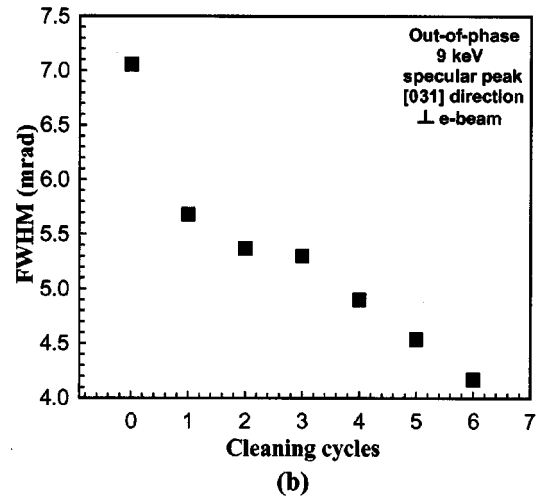


(c)

FIG. 9. (a) The RHEED intensity profiles of the split specular beam taken in the out-of-phase condition were obtained after heat cleaning at $\sim 300^\circ\text{C}$ (—) and atomic hydrogen cleaning at $\sim 380^\circ\text{C}$; (---), (- · - ·), and (—) denote the second, fourth, and sixth cleaning cycles. The split peak spacing increases with hydrogen cleaning indicating the decrease in the average terrace width. The inset is the RHEED pattern at the out-of-phase condition after hydrogen cleaning. (b) The average terrace width decreases with atomic hydrogen cleaning from $301 \pm 42 \text{ \AA}$ after heat cleaning to $229 \pm 20 \text{ \AA}$ after the sixth hydrogen cleaning cycle. Cycle 0 is heat cleaned at $\sim 300^\circ\text{C}$; 1–6 are hydrogen cleaned at $\sim 380^\circ\text{C}$. The inset gives a sketch of the terrace width of a vicinal surface. (c) The measured FWHM along the specular beam (S_{\parallel} direction).



(a)



(b)

FIG. 10. (a) Line scans across the specular beam at the out of phase condition; (---), (—), and (- · - ·) denotes to the profiles after heat cleaning, second, and sixth hydrogen cleaning cycles. (b) The measured FWHM across the specular beam (S_{\perp} direction).

cate the accuracy of determining the split peak spacing. After hydrogen cleaning cycle 6 at $\sim 380^\circ\text{C}$, the average terrace width was reduced by $\sim 20\%$, when compared to the heat-cleaned surface at $\sim 300^\circ\text{C}$. Preferential etching at terrace edges and movement of the surface atoms could have resulted in the reduced average terrace width.

When the incident electron beam is scattered from terrace edges, the diffracted specular beam width contains information on the density of kinks and meanders at the step edge. Unequal terrace widths or terrace roughness will affect the terrace periodicity and lead to broadening of the split peaks.³⁰ Line scans along the specular beam of the RHEED pattern were obtained at the out-of-phase condition. Figure 9(c) shows the FWHM in mrad along the split peak in the out-of-phase condition, after subtracting the background, as it developed with cleaning cycles. The broadening decreased from ~ 25 to ~ 8 mrad with hydrogen cleaning. In addition, line scans were taken across the specular beam as shown in Fig. 10(a). The broadening of the peak profile across the specular beam decreased with atomic hydrogen cycles compared with the heat-cleaned InP(100). The FWHM across the specular beam profile was obtained after subtracting the

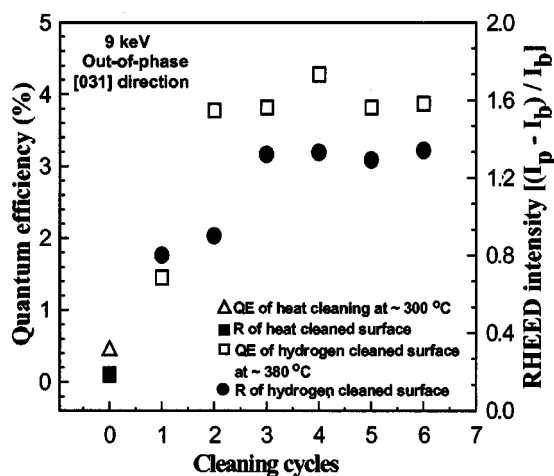


FIG. 11. Hydrogen cleaning increases the ratio $R = (I_p - I_b)/I_b$, where I_p and I_b are the RHEED peak and background intensities, respectively, measured at the out-of-phase condition. After activation to NEA, the QE correlates with the ratio R measured before activation.

background and was observed to decrease from ~ 7 to ~ 4 mrad, as shown in Fig. 10(b). The widths of the split peak decreased with hydrogen cleaning cycles, indicating a decreased kink density at the step edges.

The observed change in surface morphology from cycle 1 to 6 was accompanied by an increase in QE from 1.4% to $\sim 3.9\%$. Since the thermal cracker source produces atomic hydrogen with kinetic energy < 1 eV, no physical sputtering of surface atoms can occur; any changes in surface morphology are due to chemical etching and surface atom diffusion. Chemical etching can preferentially occur at step edges. Atomic hydrogen removed the surface contaminants, reducing the surface interfacial barrier for electron emission, thus improving the QE. Changes in the surface average terrace width do not show correlation with the measured QE. However, the RHEED intensity-to-background ratio shows good correlation with the QE of the hydrogen-cleaned InP surface as described next.

The out-of-phase RHEED intensity of the specular beam was measured before activation to NEA and this measurement was correlated to the quantum efficiency of the hydrogen-cleaned InP sample. In the out-of-phase condition, the RHEED pattern intensity is most sensitive to surface defects. Maximum intensity of the out-of-phase specular beam corresponds to a smooth clean surface, while lower intensities correspond to rougher or contaminated surfaces.³¹ In the out-of-phase condition, the ratio $R = (I_p - I_b)/I_b$, where I_p and I_b are the RHEED peak and background intensities, respectively, is inversely related to surface defect density, either roughness or contaminants.³² For a clean surface, the ratio R is a measure of adatom-vacancy density on the surface terraces. Figure 11 shows the RHEED intensity R and QE after several 3 h cleaning cycles. After hydrogen cleaning, the sample was cooled to RT, the RHEED pattern was acquired, and the QE measured after activation to NEA. The RHEED intensity was obtained several times at RT and the average values were reported. When the sample was heat-cleaned at ~ 300 °C, a RHEED intensity ratio $R \sim 0.3$ was

obtained. This surface produced a QE $\sim 0.1\%$ in response to 632.8 nm light. This indicates that the heat-cleaned InP surface is covered with contaminants expected to be hydrocarbons and native oxides. The background intensity was taken at a location between the (00) and the (01) streaks. The RHEED intensity ratio R and the QE were measured for the hydrogen-cleaned surface, where hydrogen cleaning was performed at ~ 380 °C. After the first hydrogen cleaning cycle, we obtained a RHEED intensity R of ~ 0.6 , and a QE $\sim 3.5\%$ when activated to NEA. When more hydrogen cleaning cycles were performed, the background intensity of the RHEED pattern at the out-of-phase condition decreased. The RHEED intensity R at the out-of-phase condition is a good indicator of the obtained QE after activation to NEA. The maximum specular RHEED intensity obtained for this hydrogen-cleaned surface is $R \sim 1.3$. When activated to NEA, this particular surface produced a QE of 4.3% in response to 632.8 nm light. The obtained QE is highly sensitive to the vacuum conditions and the surface preparation history.

The picture that emerges about the morphology of atomic hydrogen cleaned InP surface is a complicated one. Quantitative RHEED by itself as a surface probe gives information on average surface characteristics, such as the average terrace width and adatom-vacancy density of a clean surface. At steps, the atoms generally have lower coordination than at other surface sites and are quite reactive.¹⁹ This suggests that atomic hydrogen etching occurs preferentially at terrace edges, which causes the observed decrease of the average terrace width accompanied with an increase in terrace width fluctuation. This could be a result of a combination of thermal and chemical effects of hydrogen interaction with the surface. Thermal diffusion of atoms on the surface can also cause changes in the terrace edge morphology due to atoms diffusing and reaching sites on the terrace edge. Hydrogen ion beam smoothening of Ge(001) was previously observed and the mechanism was proposed to be both physical and chemical and could be enhanced thermally.³¹ Because of the low kinetic energy of atomic hydrogen in our case, physical sputtering effects are negligible. The RHEED peak-to-background ratio R is a good measure of adatom-vacancy concentration on the surface terraces for a clean surface. The increase in the value of R that we observe with cleaning time is due to removal of contaminants at the earlier cleaning cycles. After the surface becomes atomically clean, the ratio R becomes sensitive only to surface morphology. We observed a relatively small reduction in the average terrace width after the first hydrogen cleaning cycle along with a narrowing of the distribution of the terrace widths. While the RHEED information does not indicate the origin of that reduction, previous atomic force microscopy work on hydrogen plasma processing of GaAs(001) showed that removal of surface oxides at temperatures above 600 K led to the development of a Ga-rich surface with facet formation.³³ The relatively small reduction observed in the terrace width might be related to surface facet formation, although this occurs without apparent surface electronic quality reduction because the QE increased after the first and second hydrogen cleaning cycles at ~ 380 °C and then reached a saturation level with

further cleaning (Fig. 11). Thus, the reduction in the average terrace width observed in Fig. 9(b) is not accompanied by noticeable electronic surface quality degradation.

IV. CONCLUSION

The effect of atomic hydrogen cleaning on the morphology of the InP(100) surface was investigated and this was followed by surface activation to NEA. Atomic hydrogen cleaning produced a clean, phosphorus-stabilized (2×4)-reconstructed InP surface. InP(100) hydrogen cleaned at 385–400 °C gave a QE of ~6% after activation to NEA. The decrease in surface disorder, as determined by the RHEED background-to-peak intensity ratio $R = (I_p - I_b)/I_b$, correlated with the increased QE. A higher R surface produced higher QE. Secondary electron emission from the hydrogen-cleaned surface followed the same trends as the QE. With increased hydrogen cleaning time at 385–400 °C, surface defects due to phosphorus desorption were observed along with a reduction in QE. Thus, quantitative RHEED can be used to optimize semiconductor surface preparation prior to activation to NEA. While RHEED offers a view of surface morphology development with hydrogen cleaning and is suitable for surface probing during preparation, studies using other surface techniques are needed to resolve the nature of the microscopic reactions of atomic hydrogen with the surface and its effect on the surface electronic quality.

ACKNOWLEDGMENTS

This work was supported by the U.S. Department of Energy, Grant No. DEFG02-97ER45625.

¹D. C. Streit, in *Advance Progress of Twelfth International Conference On Indium Phosphide and Related Materials*, May 14–18, 2000 (IEEE, Williamsburg, VA), p. 11.

²Y. Chun, T. Sugaya, Y. Okada, and M. Kawabe, *Jpn. J. Appl. Phys., Part 2* **32**, L287 (1993).

³F. Ciccacci, S. DeRossi, and D. Campbell, *Rev. Sci. Instrum.* **66**, 4161 (1995).

⁴E. Petit, F. Houzay, and J. Moison, *Surf. Sci.* **269/270**, 902 (1992).

⁵T. Kikawa, I. Ochiai, and S. Takatani, *Surf. Sci.* **316**, 238 (1994).

⁶D. Gallet, G. Hollinger, and C. Santinelli, *J. Vac. Sci. Technol. B* **10**, 1267 (1992).

⁷C. M. Rouleau and R. M. Park, *J. Appl. Phys.* **73**, 4610 (1993).

⁸Z. Yu, S. L. Buczkowski, N. C. Giles, and T. H. Myers, *Appl. Phys. Lett.* **69**, 82 (1996).

⁹K. A. Elamrawi, M. A. Hafez, and H. E. Elsayed-Ali, *J. Appl. Phys.* **84**, 4568 (1998).

¹⁰W. Widdra, S. I. Yi, R. Maboudian, G. A. D. Briggs, and W. H. Weinberg, *Phys. Rev. Lett.* **74**, 2074 (1995).

¹¹E. Pehlke and P. Kratzer, *Phys. Rev. B* **59**, 2790 (1999).

¹²C. Su, C.-S. Tsai, C.-E. Lin, K.-H. Chen, J.-K. Wang, and J.-C. Lin, *Surf. Sci.* **445**, 139 (2000).

¹³N. Kondo, Y. Nanishi, and M. Fujimoto, *Jpn. J. Appl. Phys., Part 2* **31**, L913 (1992).

¹⁴G. R. Bell, N. S. Kajjaks, R. J. Dixon, and C. F. McConville, *Surf. Sci.* **401**, 125 (1998).

¹⁵J. M. Moison, Y. I. Nissim, and C. Licoppe, *J. Appl. Phys.* **66**, 3824 (1989).

¹⁶C. Licoppe, J. M. Moison, Y. I. Nissim, J. L. Regolini, and D. Bensahel, *Appl. Phys. Lett.* **53**, 1291 (1988).

¹⁷M. G. Lagally, D. E. Savage, and M. C. Tringides, in *Reflection High-Energy Electron Diffraction and Reflection Imaging of Surfaces*, edited by P. K. Larson and P. J. Dobson (Plenum, New York 1988), Vol. 188, p. 139.

¹⁸P. R. Pukite, J. M. Von Hove, and P. I. Cohen, *Appl. Phys. Lett.* **44**, 456 (1984).

¹⁹C. S. Lent and P. I. Cohen, *Surf. Sci.* **139**, 121 (1984).

²⁰I. Suemune, Y. Kunitsugu, Y. Kan, and M. Yamanishi, *Appl. Phys. Lett.* **55**, 760 (1989).

²¹R. U. Martinelli and D. G. Fisher, *Proc. IEEE* **62**, 1339 (1974).

²²C. I. Wu and A. Kahn, *J. Appl. Phys.* **86**, 3209 (1999).

²³R. U. Martinelli, *Appl. Phys. Lett.* **17**, 313 (1970).

²⁴W. Monch, *Surf. Sci.* **132**, 92 (1983).

²⁵K. A. Elamrawi, M. A. Hafez, and H. E. Elsayed-Ali, *J. Vac. Sci. Technol. A* **18**, 951 (2000).

²⁶G. W. Wicks, E. R. Rueckwald, and M. W. Koch, *J. Vac. Sci. Technol. B* **14**, 2184 (1996).

²⁷F. Ciccacci and G. Chiaia, *J. Vac. Sci. Technol. A* **9**, 2991 (1991).

²⁸W. A. Gutierrez, H. D. Pommerrenig, and S. L. Holt, *Appl. Phys. Lett.* **21**, 249 (1972).

²⁹R. U. Martinelli, M. L. Schultz, and H. F. Gossenberger, *J. Appl. Phys.* **43**, 4803 (1972).

³⁰S. A. Chalmers, A. C. Gossard, P. M. Petroff, J. M. Gaines, and H. Kroemer, *J. Vac. Sci. Technol. B* **7**, 1357 (1989).

³¹K. M. Horn, J. Y. Tsao, E. Chason, D. K. Brice, and S. T. Picraux, *J. Appl. Phys.* **69**, 243 (1991).

³²Z. H. Zhang, B. Lin, X. L. Zeng, and H. E. Elsayed-Ali, *Phys. Rev. B* **57**, 9262 (1998).

³³S. W. Robey, *Proceedings of the 45th International American Vacuum Society Symposium*, Baltimore, MD, November 2–6, 1999, p. 133.